



CHORUS

This is the accepted manuscript made available via CHORUS. The article has been published as:

Membrane morphology induced by anisotropic proteins

Kiyotaka Akabori and Christian D. Santangelo

Phys. Rev. E **84**, 061909 — Published 12 December 2011

DOI: [10.1103/PhysRevE.84.061909](https://doi.org/10.1103/PhysRevE.84.061909)

Membrane morphology induced by anisotropic proteins

Kiyotaka Akabori* and Christian D. Santangelo†

Department of Physics, University of Massachusetts, Amherst, MA 01003

There are a great many proteins that localize to and collectively generate curvature in biological fluid membranes. We study changes in the topology of fluid membranes due to the presence of highly anisotropic, curvature-inducing proteins. Generically, we find a surprisingly rich phase diagram with phases of both positive and negative Gaussian curvature. As a concrete example modeled on experiments, we find that a lamellar phase in a negative Gaussian curvature regime exhibits a propensity to form screw dislocations of definite Burgers scalar but of both chirality.

How do cells maintain and control the intricate morphologies observed in their internal membranes? By now, a number of proteins have been identified that localize to and collectively induce curvature in fluid membranes [1–3], but little is understood about connecting the individual proteins to large-scale membrane morphologies [4]. A decade of theoretical work has established only the basic principles of how proteins lead to instabilities in vesicles [5–8] and how they affect the rigidity of flat membranes [9]. Determining the resulting membrane morphology, however, remains the purview of experiment [10–12] and, sometimes, simulations [13, 14].

Recent experiments have demonstrated the ability of certain antimicrobial peptides to generate cubic, bicontinuous phases in model, lipid membranes [12]. Structures with the same symmetry, that of the Schwartz D surface, have also been observed in starved amoeba [15]. In this paper, we study changes in membrane topology due to the presence of anisotropic, curvature-inducing proteins. Our model is distinguished from much of the past theoretical work in this area by allowing both the induced curvatures and the couplings between the protein and membrane along different directions to be anisotropic. We find that magnitude *and the sign* of the induced Gaussian curvature is determined both by protein concentration and membrane rigidity. This is quite unlike the case of isotropic couplings for which the preferred mean and Gaussian curvatures are uniquely prescribed. Finally, we consider the formation of screw dislocations in a lyotropic, lamellar phase due to curvature-inducing proteins, finding a generic transition from a layered phase to an achiral defect-laden phase with screw dislocations.

I. MODEL

We formulate our model for the protein-membrane coupling by first assuming a fixed membrane shape. The second fundamental form of the neutral surface can be expressed in terms of two principal curvatures c_1 and c_2

as $h_{ij} = c_1 \mathbf{e}_{1,i} \mathbf{e}_{1,j} + c_2 \mathbf{e}_{2,i} \mathbf{e}_{2,j}$, where the \mathbf{e}_i are unit vectors along the principal curvature directions. To each protein we associate a position \mathbf{r} on the membrane and a unit vector \mathbf{u} tangent to the surface that points along the backbone (see Fig. 1). Finally, we define a unit vector $\mathbf{t} = \mathbf{u} \times \mathbf{N}$, where \mathbf{N} is the surface normal, that points transverse to the protein backbone.

The second fundamental form can be decomposed into three independent components with respect to the protein backbone: $h_{uu} = h_{ij} u^i u^j$, $h_{ut} = h_{ij} u^i t^j$ and $h_{tt} = h_{ij} t^i t^j$. Here, we are using Einstein summation convention for summing over repeated indices, and indices are raised and lowered with respect to the induced metric of the neutral surface, g_{ij} [16]. We model the interaction between membrane and protein as harmonic, allowing us to decompose the local interaction as

$$E = \frac{k_T}{2} (h_{uu} - c_L)^2 + k_X (h_{ut} - c_X)^2 + \frac{k_T}{2} (h_{tt} - c_T)^2, \quad (1)$$

where c_L and c_T are the curvatures prescribed along the longitudinal and transverse directions and c_X is related to the angle the protein backbone makes with respect to the principal directions of curvature. It is instructive to consider the case $k_T = k_X = k_T \equiv k$, for which Eq. (1) finds a condensed form

$$E = \frac{k}{2} (h_{ij} - b_{ij}) (h^{ij} - b^{ij}), \quad (2)$$

where $b_{ij} = c_L u_i u_j + c_X u_i t_j + c_T t_i t_j$. An interaction of the form of Eq. (2) has been considered by numerous authors [5, 7].

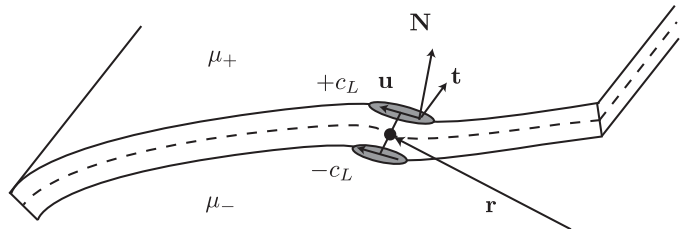


FIG. 1: Schematic model of proteins binding to a bilayer membrane, with \mathbf{u} and \mathbf{t} tangent to the membrane. If proteins bound to the top layer induce a local curvature $+c_L$ along the midsurface, an identical protein bound to the bottom surface induces a curvature $-c_L$.

*Electronic address: kakabori@physics.umass.edu

†Electronic address: csantang@physics.umass.edu

It will prove convenient to define an angle θ such that $\cos\theta = \mathbf{u} \cdot \mathbf{e}_1$, where the dot product is taken with respect to the surface metric, and dimensionless prescribed curvatures $\xi_i = c_i/|c_L|$. We further define dimensionless coupling constants $\lambda_i = k_i c_L^2/(k_B T)$. Eq. (1) now reads

$$\begin{aligned} \frac{E_{\pm}(\mathbf{r}, \theta)}{k_B T} &= \frac{\lambda_L}{2} (\xi_1 \cos^2 \theta + \xi_2 \sin^2 \theta \mp 1)^2 \\ &+ \lambda_X [(\xi_1 - \xi_2) \cos \theta \sin \theta \mp \xi_X]^2 \\ &+ \frac{\lambda_T}{2} (\xi_1 \sin^2 \theta + \xi_2 \cos^2 \theta \mp \xi_T)^2, \end{aligned} \quad (3)$$

where the sign refers to the sign of c_L .

We perform our calculations in the Grand canonical ensemble, assuming the protein binding is controlled by a chemical potential μ . We can either treat μ as a Lagrange multiplier fixing the density of proteins on the membrane or allow the proteins to reversibly bind from solution. In the latter case, μ contains a contribution from the protein binding energy and the entropy of free protein in solution. To be as general as possible, we allow the proteins to bind to either side of the membrane, observing that a protein that induces curvatures ξ_i in the midsurface when bound to one leaf of a bilayer membrane induces curvatures $-\xi_i$ when bound to the opposite leaf. We introduce different chemical potentials, μ_{\pm} , associated with either the positive or negative sign of Eq. (3), setting them equal when the proteins on one leaf are in equilibrium with those in the other. The single protein partition function is

$$Z_{\pm} = \int \frac{dA d\theta}{A_0} \exp \left\{ -\frac{E_{\pm}[\theta, \xi_1(\mathbf{r}), \xi_2(\mathbf{r})]}{k_B T} \right\}, \quad (4)$$

where dA is the area measure on the membrane midsurface and we introduce the characteristic protein area A_0 so that Z_{\pm} can be dimensionless. Since the proteins do not directly interact, the Grand partition function is

$$\Omega = \sum_{N=0}^{\infty} \sum_{M=0}^{\infty} \frac{1}{N!M!} e^{N\mu_{+}/(k_B T)} e^{M\mu_{-}/(k_B T)} Z_{+}^N Z_{-}^M. \quad (5)$$

This yields

$$\Omega = \exp \left\{ \sum_{\pm} \left[\int \frac{dA d\theta}{A_0} \exp \left(\frac{\mu_{\pm} - E_{\pm}}{k_B T} \right) \right] \right\}, \quad (6)$$

for proteins bound to either bilayer leaf.

It is straightforward to obtain the average concentration of the proteins bound to the membrane surfaces from Eq. (6) by temporarily generalizing the chemical potentials to be position and angle dependent. Then, the functional derivative of $\ln \Omega$ with respect to $\mu_{\pm}(\mathbf{r}, \theta)$ yields

$$\begin{aligned} \langle \rho_{\pm} \rangle &= k_B T \frac{\delta \ln \Omega}{\delta \mu_{\pm}(\mathbf{r}, \theta)} \\ &= A_0^{-1} \exp [(\mu_{\pm} - E_{\pm})/(k_B T)]. \end{aligned} \quad (7)$$

Finally, we note that this procedure can be generalized to multiple curvature-inducing proteins in a straightforward manner by extending the sum in Eq. (6) over each species of protein.

To relax the constraint of fixed membrane shape, we combine Eq. (6) with the Helfrich energy for a membrane, finding

$$\begin{aligned} \frac{F}{k_B T} &= \sigma A + \int dA \left[\frac{\kappa}{2} (H - H_0)^2 + \bar{\kappa} K \right. \\ &\left. - \sum_{\pm} \frac{z_{\pm}}{A_0} \int d\theta \left(e^{-E_{\pm}/(k_B T)} \right) \right], \end{aligned} \quad (8)$$

where σ is the surface tension, κ the bending modulus, $\bar{\kappa}$ the Gaussian curvature modulus, $z_{\pm} = e^{\mu_{\pm}/(k_B T)}$ the fugacity, $H = (c_1 + c_2)/2$ the mean curvature, H_0 the spontaneous curvature, $K = c_1 c_2$ the Gaussian curvature, and A the total membrane area. σ , κ , and $\bar{\kappa}$ are in units of $k_B T$. As is usual, we have introduced a membrane surface tension here. It is useful to introduce the energy of a protein on a flat membrane, $E_{\pm}^F/(k_B T) \equiv \lambda_L/2 + \lambda_X \xi_X^2 + \lambda_T \xi_T^2/2$. Adding and subtracting $2\pi e^{-E_{\pm}^F/(k_B T)}$ to Eq. (8) allows us to write

$$\begin{aligned} \frac{F}{k_B T} &= \tilde{\sigma} A + \int dA \left[\frac{\kappa}{2} (H - H_0)^2 + \bar{\kappa} K \right. \\ &\left. - \sum_{\pm} \frac{z_{\pm}}{A_0} \int d\theta \left(e^{-E_{\pm}/(k_B T)} - e^{-E_{\pm}^F/(k_B T)} \right) \right], \end{aligned} \quad (9)$$

where $\tilde{\sigma} = \sigma - \sum_{\pm} (2\pi z_{\pm}/A_0) e^{-E_{\pm}^F/(k_B T)}$. The form of Eq. (9) can be understood by expanding the energy in powers of the curvatures ξ_i . The first term is already order ξ_i ; thus, we have separated the curvature-independent effect of the proteins into an effective surface tension $\tilde{\sigma} < \sigma$. The remaining curvature-dependent contribution to the energy is responsible for selecting a local, preferred membrane curvature.

In the case we will consider here, we will assume that membrane area is fixed by treating σ as a Lagrange multiplier. In that case, it is clear that the protein contribution to the surface tension is absorbed by the Lagrange multiplier. Moreover, we will be particularly interested in proteins added to a lamellar phase, in which the surface tension term can be absorbed into the layer compression energy [17]. Since it plays no role, we will suppress it in the equations that follow to save space.

Before proceeding, it is worth noting what this procedure does not capture: the correlated fluctuations of the membrane and, by proxy, correlated fluctuations of the proteins themselves. Hence, protein interactions are only mediated by equilibrium deformations of the membrane.

II. INDUCED LOCAL CURVATURE

In order to establish our main points with minimal algebraic complication, we will mostly specialize to the extremely anisotropic case $\lambda_X = \lambda_T = 0$, with one species of protein which can bind on either leaf of the bilayer. Later, we will reintroduce the remaining couplings to see how this basic picture is modified. With this simplification, $E_{\pm}^F = e^{-\lambda_L/2}$ and $E(\mathbf{r}, \theta)/(k_B T) = \lambda_L (\xi_1 \cos^2 \theta + \xi_2 \sin^2 \theta \mp 1)/2$ in Eq. (9).

The bending modulus is shifted by

$$\Delta\kappa = \frac{\pi(z_+ + z_-)}{A_0 c_L^2} e^{-\lambda_L/2} 3(1 - \lambda_L)\lambda_L, \quad (10)$$

and the Gaussian curvature modulus is shifted by

$$\Delta\bar{\kappa} = \frac{\pi(z_+ + z_-)}{2A_0 c_L^2} e^{-\lambda_L/2} \lambda_L (\lambda_L - 1). \quad (11)$$

There is also a shift in the spontaneous curvature,

$$\Delta H_0 = 2\pi \frac{z_+ - z_-}{A_0 c_L} e^{-\lambda_L/2} \frac{\lambda_L}{\kappa + \Delta\kappa}, \quad (12)$$

which vanishes when the fugacities $z_+ = z_- = z$ are balanced. To avoid overcomplicating our analysis, we assume equal protein binding on both bilayer leaves and also zero spontaneous curvature so that $\Delta H_0 = H_0 = 0$.

There are two distinct regimes of behavior to consider. When $\lambda_L < 1$, the membrane becomes more rigid with increasing protein concentration. For $\lambda_L > 1$, on the other hand, the membrane softens with increasing protein concentration. Qualitatively similar behavior has been calculated for the case of isotropic couplings [9]. This softening eventually leads to an instability with respect to *continuous* perturbations at a critical protein fugacity $(z_+ + z_-)/(A_0 \kappa c_L^2) > e^{\lambda_L/2}/[3\pi\lambda_L(\lambda_L - 1)]$ in which $\kappa + \Delta\kappa < 0$.

Topological instabilities occur when either of the two ‘‘topological moduli’’, $\kappa_+ = \kappa/2 + \bar{\kappa}$ and $\kappa_- = -\bar{\kappa}$, become negative [18, 19]. When $\kappa_+ < 0$, the membrane becomes unstable to topological rearrangements that induce positive Gaussian curvature, for example to spherical vesicles [19]. Similarly, when $\kappa_- < 0$, the membrane becomes unstable toward the formation of negative Gaussian curvature, which has been implicated in the transition from an L_α to an L_3 phase in lamellar systems [19]. In terms of the original bare moduli, we find that $\kappa_+ < 0$ when

$$\frac{z_+ + z_-}{A_0 c_L^2} > 4 \frac{e^{\lambda_L/2}}{\pi\lambda_L(\lambda_L - 1)} \left(\frac{\kappa}{2} + \bar{\kappa} \right), \quad (13)$$

and $\kappa_- < 0$ when

$$\frac{z_+ + z_-}{A_0 c_L^2} > 2 \frac{e^{\lambda_L/2}}{\pi\lambda_L(\lambda_L - 1)} |\bar{\kappa}|. \quad (14)$$

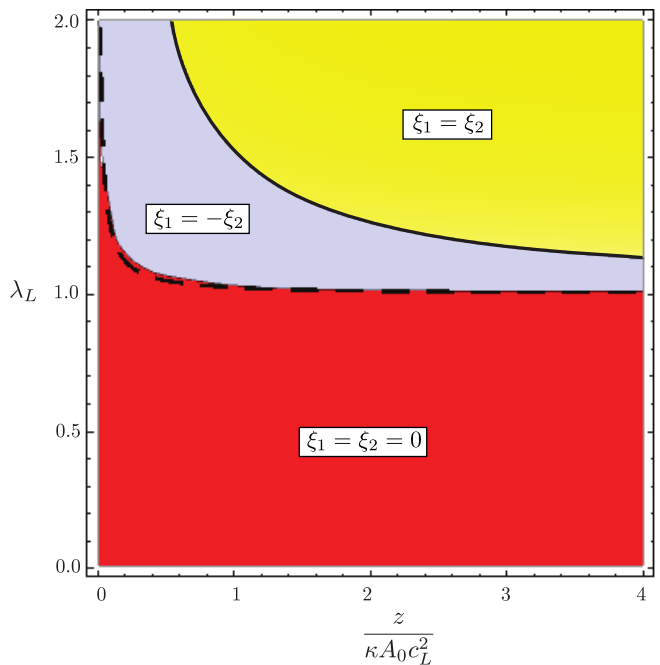


FIG. 2: (color online) $[z/(\kappa A_0 c_L^2), \lambda_L]$ phase diagram for a single species with equal binding to both leaves and $\lambda_X = \lambda_T = 0$. We’ve chosen $\bar{\kappa} = -0.05\kappa$. The dashed line is the stability line of Eq. (11) between the flat phase labelled $\xi_1 = \xi_2 = 0$ (red) and the minimal surface phase labelled $\xi_1 = -\xi_2$ (blue). The spherical phase is labelled $\xi_1 = \xi_2$ (yellow), with a transition from the $K < 0$ phase that is first order. Intensity of color indicates the magnitude of the Gaussian curvature, which is nearly constant.

To study the topological phase diagram more concretely, we ask the question: what combinations of membrane curvatures ξ_1 and ξ_2 minimize the free energy *locally*, that is, the free energy density given by the integrand in Eq. 9? A typical *local* phase diagram as a function of λ_L and fugacity z is shown in Fig. 2. We generically find three phases: a flat membrane with boundary given by Eq. (14), a saddle phase with $\xi_1 = -\xi_2 \leq 1$, and a spherical phase with $\xi_1 = \xi_2 \leq 1$. There is a weak dependence of the induced curvature on the protein fugacity. When $\bar{\kappa} = 0$, the transition from flat to minimal surface phase occurs along the line $\lambda_L = 1$ as predicted by Eq. (11). For $\bar{\kappa} < -\kappa/3$, the transition from the flat phase proceeds directly to spheres, as can also be seen from Eqs. (13) and (14). Why do anisotropic couplings lead to such rich phase diagrams? When $\lambda_X = \lambda_T = 0$, the protein curvature can be accommodated by both $K > 0$ and $K < 0$ since they need only find a single direction in which the membrane curvature is commensurate with the protein’s prescribed curvature. However, the orientational entropy of the protein is maximized at umbilics ($\xi_1 = \xi_2$) while the bending energy is minimized at minimal surfaces ($\xi_1 = -\xi_2$). The dependence on the combination z/κ arises directly from this competition.

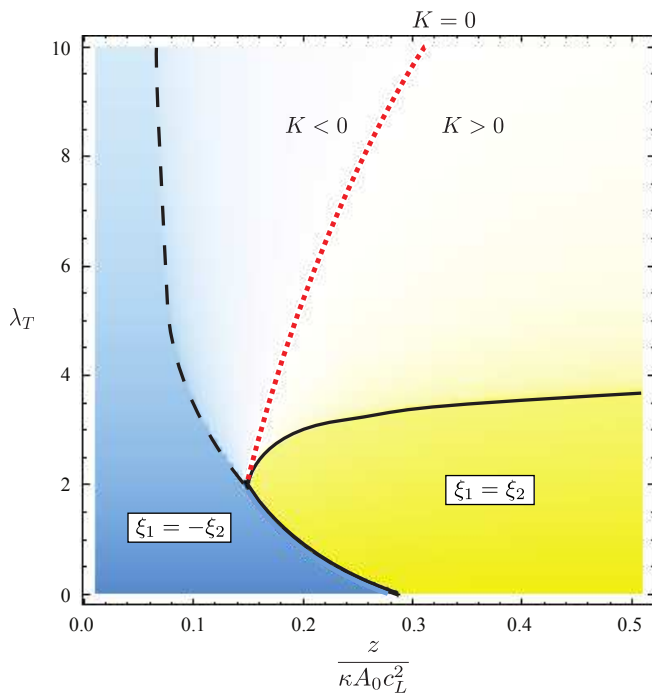


FIG. 3: (color online) $[z/(\kappa A_0 c_L^2), \lambda_T]$ phase diagram ($\bar{\kappa} = 0$) for a single species of protein with $\lambda_X = \lambda_L = 10$ and with equal binding to both bilayer leaves. The solid, black lines indicate a discontinuous transition while the dashed, black line is continuous. There is a change of symmetry across each of these black lines. Cylinders ($K = 0$) lie on the dotted, red line. The (gray) color intensity indicates the magnitude of the Gaussian curvature.

If we introduce the coupling $\lambda_X \neq 0$, the qualitative phase diagram of Fig. 2 changes only by increasing the area of stability for flat membranes at the expense of the $K < 0$ phase. This holds true even when $\lambda_X = \lambda_L$. For $\lambda_T \neq 0$, however, the phase diagram changes qualitatively. For concreteness, assume $\xi_T = 0$ so that the protein induces local cylindrical curvature. A cross-section of the phase diagram in the (λ_T, z) plane is shown in the slice $\lambda_L = \lambda_X = 10$ in Fig. 3. We see not only the saddle and spherical phases but two regions of nearly cylindrical structures, one with $K < 0$ and one with $K > 0$. The transitions meet at a single critical point at which $\xi_1 = \xi_2 = 0$. When $\lambda_T = \lambda_X = \lambda_L = 10$, however, the membrane is cylindrical at nearly all fugacities with only a small deviation toward a saddle at very low densities. This propensity to form saddles at small fugacity disappears at smaller values the couplings. At $\lambda_L = \lambda_X = \lambda_T = 3$, for example, there is only a flat phase at low fugacity and a cylindrical phase at high fugacity.

III. SCREW DISLOCATIONS IN LAMELLAR PHASES

In this section, we use the model of anisotropic proteins to explore the transition from a lamellar phase to

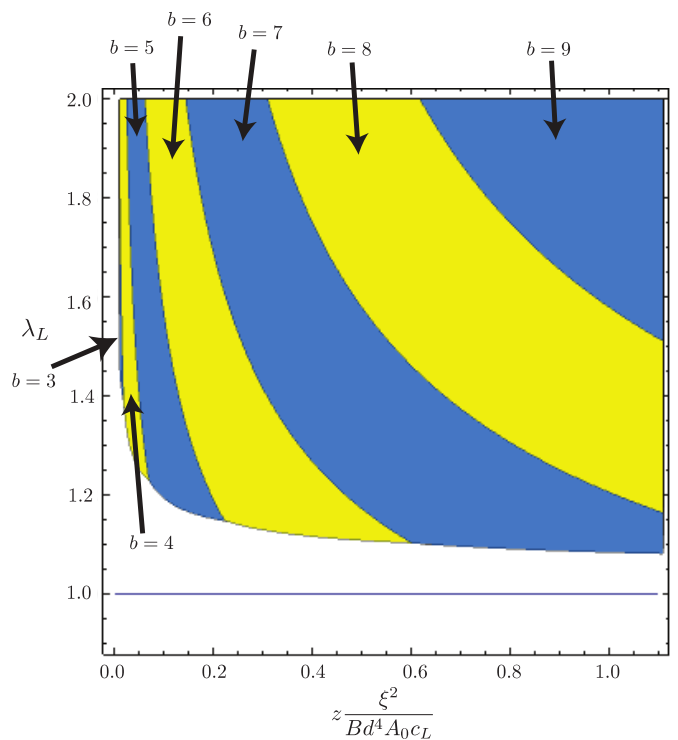


FIG. 4: (color online) $[z\xi^2/(Bd^4 A_0 c_L), \lambda_L]$ critical line above which helicoids are energetically favorable for $\bar{\kappa} = 0$. The flat phase is stable in the region $\lambda_L < 1$. Color (shading) is added as a guide to the eye.

one with complex topology. We again focus on the prototypical case that $\lambda_X = \lambda_T = 0$ and $\bar{\kappa} = 0$, for which there is only a spherical and a saddle phase (when $\lambda_L > 1$) (see Fig. 2). In the case of the spherical phase, the lowest energy state is one of monodisperse spherical vesicles of radius c_L^{-1} .

In the saddle phase, however, the lowest energy state occurs when $H = 0$ and K is given by the prescribed Gaussian curvature ($\xi_1 = -\xi_2 \approx 1$). This is impossible in a three dimensional Euclidean space; the membrane energy is frustrated by the constraints of geometry. However, lamellar phases with a sufficiently strong preference for negative Gaussian curvature can develop a variety of complex, but ordered, morphologies [21]. A layered structure with the same topology as the Schwartz D surface, the structure most commonly observed with a variety of negative Gaussian curvature inducing proteins [12], can be obtained through a lattice of screw dislocations through Schnerk's first surface [22]. Using it as a guide, we consider the insertion of a screw dislocation into a lamellar phase as a prototype of a topological transition driven by proteins.

In the absence of proteins, a screw dislocation is described by a helicoid which has $K < 0$ everywhere. We will assume this form is a good description of a screw dislocation in the presence of proteins as well. In terms of coordinates (x, y) on a flat reference layer, the multi-

valued height function,

$$h(x, y) = \left(\frac{b}{2\pi}\right) \tan^{-1}\left(\frac{y}{x}\right), \quad (15)$$

where $b = nd$ is the Burgers scalar, n an integer and d the layer spacing, is an extremum of both the bending and compression energies [20]. Screw dislocations have a large elastic contribution to their line tension, arising from the deviation from the equilibrium layer spacing near the core, of the form $\tau = Bb^4/(256\pi^4\xi^2)$, where B is the bulk modulus and ξ is a microscopic core size [20]. Due to the divergence in τ as $\xi \rightarrow 0$, we neglect other contributions to the core energy.

Since $H = 0$, this line tension must be balanced with the contribution from Eq. (9) if screw dislocations are energetically favorable. We evaluate Eq. (9) numerically. We find that a screw dislocation becomes energetically favorable when compared to the flat phase above the critical line shown in Fig. 4. Increasing fugacity prefers an increasing Burgers scalar, with both chiralities degenerate. Since this surface is not of the optimal curvature everywhere, this critical line occurs at larger λ_L than predicted by the local phase diagram. The transition also depends strongly on the bulk modulus of the lamellar phase, though we note that the layer spacing is typically set by $d \sim \sqrt{(\kappa/d)/B}$ [20]. If we use $\xi \sim d$ for the core size we obtain that $z\xi^2/(Bd^4A_0c_L) \sim zc_Ld/(\kappa A_0c_L^2)$, so the horizontal axis of Fig. 4 is roughly comparable to that of our local phase diagrams when $c_L \sim 1/d$. Finally, we note that, once it is energetically favorable to insert a screw dislocation, screw dislocations will proliferate. The result will be a defect-laden phase with either an ordered or disordered arrangement of screw dislocations.

IV. DISCUSSION AND SUMMARY

In this paper, we have studied topological transitions in membranes induced by anisotropic, curvature-inducing proteins. It was already anticipated by Fournier [5] that anisotropic proteins can favor negative Gaussian curva-

ture at certain densities. Indeed, when the three elastic moduli coupling the proteins to the membrane are equal – that is, the proteins induce a local, anisotropic membrane curvature *isotropically* – we indeed recover this result. Nevertheless, we have found that, once the three elastic moduli differ, anisotropic proteins can induce both positive and negative Gaussian curvatures no matter what their intrinsic curvatures are. In fact, the curvature induced depends on the protein densities and membrane moduli, and arise from a competition between protein entropy and membrane curvature. We also identify the dimensionless parameters that govern the minimal energy *local* curvature, which depend on a combination of membrane rigidity and protein area fraction. Consequently, should curvature-inducing proteins take advantage of our mechanism for sculpting membranes, tuning the membrane moduli by adding cosurfactants or changing lipid mixtures can induce a transition from negative to positive Gaussian curvature.

Beyond this, we consider large scale re-arrangements of a fluid membrane due to proteins that favor the formation of negative Gaussian curvature. The inherent frustration of surfaces with negative Gaussian curvature – because they cannot satisfy the local, lowest-energy curvature everywhere – modifies the location of the transition. At this slightly higher threshold, we predict a transition from a lamellar phase to one with screw dislocations. Since dislocations of both chirality should appear with equal probability, the resulting phase will be achiral. In fact, a lattice of parallel, opposite screw dislocations forms a phase with Pn3m symmetry [22], which have been observed in experiments in which anisotropic proteins have been added to a lipid mixture [10].

Finally, we have neglected membrane shape fluctuations in our analysis. These fluctuations will induce additional correlations in the protein positions. Whether this will qualitatively change the phase diagram remains to be seen.

This work was funded by the National Science Foundation through DMR-0846582 and by the University of Massachusetts Amherst.

-
- [1] Brian J. Peter, Helen M. Kent, Ian G. Mills, Yvonne Valis, P. Jonathan G. Butler, Philip R. Evans, and Harvey T. McMahon, *Science* **303**, 495 (2004).
 - [2] R. F. Epand, J. Martinou, S. Montessuit, R. M. Epand, and C. M. Yip, *Biomed. Biophys. Res. Comm.* **298**, 744 (2002)
 - [3] Y. Feng, L. Zhang, T. Hu, X. Shen, J. Ding, K. Chen, H. Jiang, and D. Liu, *Arch. Biochem. Biophys.* **484**, 46 (2009).
 - [4] H.T. McMahon and J.L. Gallop, *Nature* **438**, 590 (2005).
 - [5] J.B. Fournier, *Phys. Rev. Lett.* **76**, 4436 (1996)
 - [6] P.G. Dommersnes and J.P. Fournier, *Biophys. J.* **83**, 2898 (2002).
 - [7] M. Fošnarič, A. Igič, T. Slivnik and V. Kralj-Iglič, *Advances in Planar Lipid Bilayers and Liposomes (vol. 8), Ed. A.L. Liu, Chapter 6* (Elsevier, New York, 2008).
 - [8] V. Kralj-Iglic, V. Heinrich, S. Svetina and B. Zeks, *Eur. Phys. J. B* **10**, 5 (1999).
 - [9] M. Fosnarič, A. Iglič, and S. May, *Phys. Rev. E* **74**, 051503 (2006).
 - [10] L. Yang, V. D. Gordon, D. R. Trinkle, N. W. Schmidt, M. A. Davis, C. DeVries, A. Som, J. E. Cronan, Jr., G. N. Tew, and G. C. L. Wong, *Proc. Nat. Acad. Sci.* **105**, 20595 (2008)
 - [11] L. Yang, V. D. Gordon, A. Mishra, A. Som, K. R. Purdy, M. A. Davis, G. N. Tew, and G. C. L. Wong, *J. Am.*

- Chem. Soc. **129**, 12141 (2007).
- [12] A. Mishra, V. D. Gordon, L. Yang, R. Coridan, and G. C. L. Wong, *Angew. Chem. Int. Ed.* **47**, 2986 (2008).
- [13] B. J. Reynwar, G. Illya, V. A. Harmandaris, M. M. Müller, K. Kremer, and M. Deserno, *Nature* **447**, 461 (2007).
- [14] G. S. Ayton, E. Lyman, V. Krishna, R. D. Swenson, C. Mim, V. M. Unger, G. A. Voth, *Biophys. J.* **97**, 1616 (2009).
- [15] Y. Deng, M. Marko, K. F. Buttler, A. Leitha, M. Mieczkowski, and C. A. Mannella, *J. Struct. Bio.* **127**, 231 (1999).
- [16] M. P. do Carmo, *Differential Geometry of Curves and Surfaces* (Prentice-Hall, Englewood Clis, 1976).
- [17] L. Golubović and T.C. Lubensky, *Phys. Rev. B* **39**, 12110 (1989).
- [18] W. Helfrich, in *Physics of Defects, Les Houches Summer School. Balian, R., M. Kleman, J.-P. Poirier, eds.* (North Holland, Amsterdam, 1980).
- [19] D.C. Morse, *Phys. Rev. E* **50**, R2423 (1994).
- [20] P.G. de Gennes and J. Prost, *The physics of liquid crystals* (Oxford University Press, Oxford, 1995).
- [21] B.A. DiDonna and R.D. Kamien, *Phys. Rev. Lett.* **89**, 215504 (2002).
- [22] C.D. Santangelo and R.D. Kamien **96**, 137801 (2006).